Brazilian Journal of Physics
ISSN: 0103-9733
luizno.bjp@gmail.com
Sociedade Brasileira de Física
Brasil

Ghanbari-Adivi, Ebrahim
A Self-Consistent Model for Positronium Formation from Helium Atoms
Brazilian Journal of Physics, vol. 42, núm. 3-4, julio-diciembre, 2012, pp. 172-179
Sociedade Brasileira de Física
Sâo Paulo, Brasil

Available in: http://www.redalyc.org/articulo.oa?id=46423465002

How to cite
Complete issue
More information about this article
Journal's homepage in redalyc.org

Scientific Information System
Network of Scientific Journals from Latin America, the Caribbean, Spain and Portugal
Non-profit academic project, developed under the open access initiative

Braz J Phys (2012) 42:172–179
DOI 10.1007/s13538-012-0080-3

SBF SOCIEDADE BRASILEIRA DE FÍSICA

ATOMIC PHYSICS

A Self-Consistent Model for Positronium Formation from Helium Atoms

Ebrahim Ghanbari-Adivi

Received: 31 July 2011 / Published online: 18 May 2012
© Sociedade Brasileira de Física 2012

Abstract The differential and total cross sections for electron capture by positrons from helium atoms are calculated using a first-order distorted wave theory satisfying the Coulomb boundary conditions. In this formalism, a parametric potential is used to describe the electron screening in a consistent and realistic manner. The present procedure is self-consistent because (a) it satisfies the correct boundary conditions and post–prior symmetry, and (b) the potential and the electron binding energies appearing in the transition amplitude are consistent with the wave functions describing the collision system. The results are compared with the other theories and with the available experimental measurements. At the considered range of collision energies, the results agree reasonably well with recent experiments and theories.

Keywords Distorted-wave approximation · Positronium formation · Coulomb boundary conditions · Differential and total cross sections

1 Introduction

Both positrons (e^+) and positronium atoms (Ps) have important applications in many different branches of physics, chemistry, and other fields [1–6]. This has motivated numerous studies of collisions in which electrons in atomic or molecular targets are captured by positrons [7–26]. In a collision, each of the various modes into which the system under study may be fragmented is called a channel. For definiteness, consider the positron–helium scattering system, on which the present paper is focused. In the entrance channel of the $e^+ + \mathrm{He}$ system, the positron impacts on the helium atom. The exit channel can be one of a number of possible fragmentations, such as elastic or excitation scattering ($e^+ + \mathrm{He}$ and/or $e^+ + \mathrm{He}^*$), positronium formation ($\mathrm{Ps} + \mathrm{He}^+$), or ionization ($e^+ + e^- + \mathrm{He}^*$). An exit channel is said to be open if the corresponding collision is allowed by all known conservation laws, such as energy and momentum conservation; otherwise, it is said to be closed. Since the transition amplitude in general is a function of the energy, the occurrence probability for each open channel depends on the impact energy of the projectile. The transition probabilities per unit time, per unit target scatterer, and per unit of the flux of incident particles with respect to the target are called the cross sections. Experiments measure cross sections, while theoretical studies usually attempt to compute them. In positron–helium collisions, since the charge transfer process amounts to a four-body problem, the theoretical investigation of the rearrangement involves the full complexities of the quantum mechanical four-body problem and as such is too difficult to be exactly solved.

Notwithstanding the difficulty, numerous theoretical investigations are found in the literature [17–19, 27–34], along with experimental studies [14, 35–40]. Most of the theories were formulated within a single active electron picture. In this formalism, it is important to provide a consistent and realistic treatment of the passive electron screening effects in order to satisfy the

E. Ghanbari-Adivi (✉)
Department of Physics and Isfahan Quantum Optics Group(IQOG), Faculty of Science, University of Isfahan, Isfahan 81746-73441, Iran
e-mail: ghanbari@phys.ui.ac.ir

Coulomb boundary conditions and post–prior equivalency and to make the wave functions, binding energies, and Coulomb phase factors consistent with each other.

In the context of K-shell electron capture processes by fast protons from multielectron atoms, Decker and Eichler [41] have discussed the deviations of a few of the standard formalisms from these constraints in some detail. They adopted a parameterized potential due to Green et al. [42, 43], the Green–Sellin–Zachor (GSZ) potential, to construct a self-consistent screened boundary-corrected first-Born approximation theory for calculation of the K-shell electron capture total cross sections in collisions of proton with helium and carbon as well as collision of alpha particles with lithium atoms.

In the present paper, a distorted-wave boundary-corrected first-order Born (DWB1B) formalism accompanied by the GSZ potential is applied to obtain a satisfactory description of positronium formation in positron–helium atom collisions at intermediate energies. In this model, the single-zeta Hartree–Fock wave function and its corresponding binding energy, which shows very good agreement with those for GSZ potential, describes the initial bound state of the electron. Consequently, the wave function and the corresponding energy in the post or prior formalisms are the eigenfunction and eigenenergy of the same effective screening potential that appears explicitly in the corresponding amplitudes. Thus, in addition to satisfying both the Coulomb boundary conditions and post–prior symmetry, the wave functions, binding energies, and Coulomb phase factors are consistent with each other.

The plan of the paper is as follows. Section 2 outlines the formalism. Section 3 presents and discusses the results and compares them with other theories and experimental data. The concluding remarks and a summary comprise the last section. Unless otherwise stated, atomic units are used throughout.

2 Theory

Consider a bare ion P with mass M_P and charge Z_P impingent on an atomic target composed of an active electron e and a residual target-ion T with masses m and M_T, respectively. During the collision, the projectile captures the electron. According to the time-independent boundary-corrected perturbation formalism of electron capture developed by Toshima et al. [44] and Belkić et al. [45], the DWB1B amplitude for such a process has the prior and post forms

$$\mathcal{A}^{(\mathrm{prior})}_{\mathrm{DWB1B}} = \langle \chi_f \left| (V_\mathrm{i} - V_\mathrm{i}^\infty) \right| \chi_\mathrm{i} \rangle \tag{1}$$

and

$$\mathcal{A}^{(\mathrm{post})}_{\mathrm{DWB1B}} = \langle \chi_\mathrm{f} \left| (V_\mathrm{f} - V_\mathrm{f}^\infty) \right| \chi_\mathrm{i} \rangle, \tag{2}$$

where V_i^∞ and V_f^∞ are the asymptotic limits of the distorting potentials V_i and V_f in initial and final channels. In position space, the corresponding distorted-wave functions χ_i and χ_f are given by the equalities

$$\chi_\mathrm{i}(\mathbf{r}_T, \mathbf{R}_T, \mathbf{R}) = \phi_i(\mathbf{r}_T) \exp(i\mathbf{K_i} \cdot \mathbf{R}_T) \times \exp\left(i \frac{Z_P (Z_T^a - 1)}{\mathrm{v_i}} \ln(\mathrm{v_i} R - \mathbf{v_i} \cdot \mathbf{R}) \right) \tag{3}$$

and

$$\chi_\mathrm{f}(\mathbf{r}_P, \mathbf{R}_P, \mathbf{R}) = \phi_\mathrm{f}(\mathbf{r}_P) \exp(i\mathbf{K_f} \cdot \mathbf{R}_P) \times \exp\left(i \frac{Z_T^a (Z_P - 1)}{\mathrm{v_f}} \ln(\mathrm{v_f} R - \mathbf{v_f} \cdot \mathbf{R}) \right), \tag{4}$$

in which $\phi_i(\mathbf{r}_T)$ and $\phi_f(\mathbf{r}_P)$ are the initial and final bound-state electronic wave functions. In (3) and (4), the plane wave functions describe the heavy-particle motion in the entrance and exit channels, and the phase factors ensure that the overall solutions satisfy the proper asymptotic boundary conditions for the distorting potentials. In these equations, $\mathbf{r}_P$ and $\mathbf{r}_T$ are the electron coordinates relative to the projectile and target nucleus, respectively, $\mathbf{R}_P$ is the position vector of the center of mass of the Pe subsystem relative to T, $\mathbf{R}_T$ is a similar vector directed from the center of mass of the Te subsystem to P, and $\mathbf{R}$ is the internuclear coordinate vector directed from T to P. The bare projectile and the asymptotic target-ion charges are Z_P and Z_T^a, respectively, $\mathbf{v}_\mathrm{i}$ and $\mathbf{v}_\mathrm{f}$ are the projectile velocity in the initial channel and resultant bound subsystem velocity in the final channel, respectively, and $\mathbf{K}_\mathrm{i}$ and $\mathbf{K}_\mathrm{f}$ are the wave vectors describing the relative motions in the two channels.

The Coulomb interaction between the active electron and the projectile ion is denoted $V_{Pe}(\mathbf{r}_P) = -Z_P/r_P$, with the asymptotic form of $V_{Pe}^\infty(\mathbf{R}) = -Z_P/R$. We take the internuclear potential to be that of a bare nucleus screened by the nonactive electrons represented by *frozen* orbitals. For this purpose, the parameterized potential obtained by Green et al. [42, 43] is adequate because it has the correct behavior near the nucleus and at infinity and because it yields orbital binding energies and wave functions in good agreement with the corresponding Hartree–Fock results [46]. Within a single active electron model, using the GSZ potential for a neutral atom, one can write the

projectile–target interaction in coordinate representation $V_{PT}(\mathbf{R})$ as

$$V_{PT}(R) = \frac{Z_P}{R}\left[1 + (Z_T - 1)\Omega(R)\right], \tag{5}$$

where Z_T is the nuclear charge of the multielectron atomic target and $\Omega(R)$ is given by the expression

$$\Omega(R) = \frac{1}{1 - H[1 - \exp(R/\mathrm{d})]}. \tag{6}$$

Optimized values for the characteristic parameters H and d have been given by Szydlik and Green [43] for $Z_T \leq 18$. Near the nucleus, the projectile ion feels the bare nuclear charge Z_T; while at large distances, the potential behaves as Z_P/R corresponding to the residual singly charged ion.

With the potential (5), the post and prior amplitudes (1) and (2) satisfy the appropriate boundary conditions in the initial and final channels. It is easy to see that the two amplitudes are identical provided that $\phi_i(\mathbf{r}_T)$ and $\phi_f(\mathbf{r}_P)$ be the exact solutions of the atomic Schrödinger equations associated with the potentials $V_{Te}(\mathbf{r}_T)$ and $V_{Pe}(\mathbf{r}_P)$, respectively. The wave functions, binding energies, and Coulomb phase factors are moreover consistent with each other. Hereafter, given the equivalence between the prior and post wave functions, we will omit the superscripts *post* and *prior* in (1) and (2) and write $\mathcal{A}_{\mathrm{DWB1B}}$ to denote the amplitudes.

The Fourier transform of the V_{PT} potential can be written in the form

$$\tilde{V}_{PT}(\mathbf{k}) = \sqrt{\frac{2}{\pi}}\frac{Z_P}{k^2} + \sqrt{\frac{2}{\pi}} Z_P(Z_T - 1)\tilde{\mathcal{V}}(k), \tag{7}$$

where

$$\tilde{\mathcal{V}}(k) = \frac{1}{k}\int_0^\infty \mathrm{d}R\,\Omega(R)\sin(kR). \tag{8}$$

With the given interaction potentials, $V_{Pe}(\mathbf{r}_P)$ and $V_{PT}(\mathbf{R})$, the transition amplitude for electron capture comprises three terms:

$$\mathcal{A}_{\mathrm{DWB1B}} = \mathcal{A}_1 + \mathcal{A}_2 + \mathcal{A}_3, \tag{9}$$

with the following explicit expressions for the partial amplitudes $\mathcal{A}_1$, $\mathcal{A}_2$ and $\mathcal{A}_3$ in coordinate representation:

$$\begin{aligned}
\mathcal{A}_1 &= -Z_P \int \mathrm{d}\mathbf{r}_P \mathrm{d}\mathbf{R}_P \chi_{\mathrm{f}}^*(\mathbf{r}_P, \mathbf{R}_P, \mathbf{R}) \frac{1}{r_P} \chi_{\mathrm{i}}(\mathbf{r}_T, \mathbf{R}_T, \mathbf{R}) \\
\mathcal{A}_2 &= +Z_P \int \mathrm{d}\mathbf{r}_P \mathbf{R}_P \chi_{\mathrm{f}}^*(\mathbf{r}_P, \mathbf{R}_P, \mathbf{R}) \frac{1}{R} \chi_{\mathrm{i}}(\mathbf{r}_T, \mathbf{R}_T, \mathbf{R}) \\
\mathcal{A}_3 &= Z_P(Z_T - 1) \int \mathrm{d}\mathbf{r}_P \mathrm{d}\mathbf{R}_P \chi_{\mathrm{f}}^*(\mathbf{r}_P, \mathbf{R}_P, \mathbf{R}) \frac{\Omega(R)}{R} \\
&\quad \times \chi_{\mathrm{i}}(\mathbf{r}_T, \mathbf{R}_T, \mathbf{R}).
\end{aligned} \tag{10}$$

We now consider the special case $Z_P = 1$ and the transition from an initial $1s$ hydrogen-like state such as $\phi_i(\mathbf{x}_T) = N_T \exp(-\zeta_T x_T)$ to a final $1s$ hydrogen-like state of form $\phi_f(\mathbf{x}_P) = N_P \exp(-\zeta_P x_P)$, where N_P and N_T are normalization factors. We apply the Scrödinger equation for the final bound subsystem, use the Fourier transform analysis, and evaluate the resulting integrals to obtain the following expression for the first partial amplitude, $\mathcal{A}_1$:

$$\begin{aligned}
\mathcal{A}_1 &= -16\pi^2 N_P N_T Z_P \left(\frac{K^2}{2\mu_f} - \epsilon_f\right) \\
&\quad \times \frac{\partial^2}{\partial\zeta_P \partial\zeta_T}\left[\frac{1}{(K^2 + \zeta_P^2)(J^2 + \zeta_T^2)}\right],
\end{aligned} \tag{11}$$

where $\mu_f = M_P m/(M_P + m)$ is the reduced final-state mass of the bound subsystem, and $\mathbf{J}$ and $\mathbf{K}$ are the momenta transferred to the target ion and the projectile, respectively, during the collision.

Similarly, using the Fourier transform techniques and Lewis integral [47], we derive the following closed form for the second partial amplitude $\mathcal{A}_2$:

$$\begin{aligned}
\mathcal{A}_2 &= 8\pi^2 N_P N_T Z_P \\
&\quad \times \frac{\partial^2}{\partial\zeta_P \partial\zeta_T}\left[(\alpha^2 - \beta)^{-1/2} \ln\left[\frac{\alpha + (\alpha^2 - \beta)^{1/2}}{\alpha - (\alpha^2 - \beta)^{1/2}}\right]\right],
\end{aligned} \tag{12}$$

with

$$\alpha = (K^2 + \zeta_P^2)\zeta_T + (J^2 + \zeta_T^2)\zeta_P$$

and

$$\beta = (K^2 + \zeta_P^2)(J^2 + \zeta_T)[v_f^2 + (\zeta_P^2 + \zeta_T^2)].$$

Finally, we use Fourier analysis to write the third partial amplitude $\mathcal{A}_3$ in the form

$$\mathcal{A}_3 = 8\pi^2 N_P N_T Z_P(Z_T - 1)\frac{\partial^2}{\partial\zeta_P \partial\zeta_T}\mathcal{I}(\zeta_P, \zeta_T), \tag{13}$$

where

$$\mathcal{I}(\zeta_P, \zeta_T) = \frac{1}{\pi^2}\int \mathrm{d}\mathbf{k}\frac{\tilde{\mathcal{V}}(k)}{|(\mathbf{k} - \mathbf{K}|^2 + \zeta_P^2)(\mathbf{k} + \mathbf{J}|^2 + \zeta_T^2)}. \tag{14}$$

Before numerical calculations become possible, we have to analytically simplify the right-hand side of (13). To this end, noticing that $\tilde{\mathcal{V}}(k)$ is a radial function, we

use Feynman's identity [48] to evaluate the angular integral over **k**:

$$\mathcal{I}(\zeta_P,\zeta_T) = -\frac{1}{\pi}\int_0^1 \frac{\mathrm{d}x}{\gamma}\int_0^\infty \mathrm{d}R\Omega(R) \times \int_{-\infty}^{+\infty} \mathrm{d}k \frac{\sin(kR)}{k^2+2\gamma k+\delta}, \tag{15}$$

where

$$\gamma = \sqrt{J^2(1-x)^2 + K^2x^2 - 2x(1-x)\mathbf{J}\cdot\mathbf{K}},$$

and

$$\delta = (J^2+\zeta_T^2)(1-x) + (K^2+\zeta_P^2)x.$$

Next, we apply Cauchy's residue theorem to the last integral on the right-hand side of (15) to see that

$$\int_{-\infty}^{+\infty} \mathrm{d}k \frac{\sin(kR)}{k^2+2\gamma k+\delta} = -\frac{\pi}{\sqrt{\delta-\gamma^2}} \mathrm{e}^{-R\sqrt{\delta-\gamma^2}} \sin(\gamma R). \tag{16}$$

With this, we have reduced the four-dimensional integral $\mathcal{I}(\zeta_P,\zeta_T)$ in (14) to a two-dimensional form,

$$\mathcal{I}(\zeta_P,\zeta_T) = \int_0^1 \frac{\mathrm{d}x}{\gamma\sqrt{\delta-\gamma^2}} \int_0^\infty \mathrm{d}R\Omega(R)\mathrm{e}^{-R\sqrt{\delta-\gamma^2}}\sin(\gamma R), \tag{17}$$

which can be easily computed numerically, along with the derivatives on the right-hand side of (13).

For single-electron capture in impact of positron on helium atoms $Z_T = 2.0$, $\epsilon_i = -0.89648$, $\epsilon_f = -0.25$, $\mu_f = 0.5$, $\zeta_P = 0.5$, $\zeta_T = 1.6875$, $N_P = \zeta_P\sqrt{\zeta_P/\pi}$, $N_T = \zeta_T\sqrt{\zeta_T/\pi}$, and the corresponding differential and total cross sections are given by

$$\sigma(\theta) = \frac{\mathrm{d}\sigma}{\mathrm{d}\Omega} = \frac{2}{\pi^2}\frac{v_f}{vi}|\mathcal{A}_{\mathrm{DWB1B}}|^2, \tag{18}$$

and

$$\sigma_{\mathrm{Total}} = 2\pi\int_0^\pi \sigma(\theta)\sin\theta\mathrm{d}\theta, \tag{19}$$

respectively.

In order to account for the excited final states, we multiply the right-hand side of (19) by 1.202, according to the Oppenheimer n^{-3} scaling rule [49].

3 Results and Conclusions

We now present the computed differential and total cross sections for positronium formation in positron collisions with helium atoms and compare them with other theoretical approaches and experimental data. In order to evaluate the third partial transition amplitude, $\mathcal{A}_3$, we rely on the Gaussian quadrature method to compute the two-dimensional integral $\mathcal{I}(\zeta_P,\zeta_T)$ in (17).

Figure 1 shows the angular differential cross sections for positronium formation at three incident energies, 100, 200, and 500 eV. All three curves display a dip due to the cancelation between the contributions of the attractive and repulsive interactions to the first-order transition amplitude. A similar, unphysical dip has been found in a first-order Born treatment of electron capture in the collision of a proton with hydrogen atoms [50]. Figure 1a, b compare our results with those

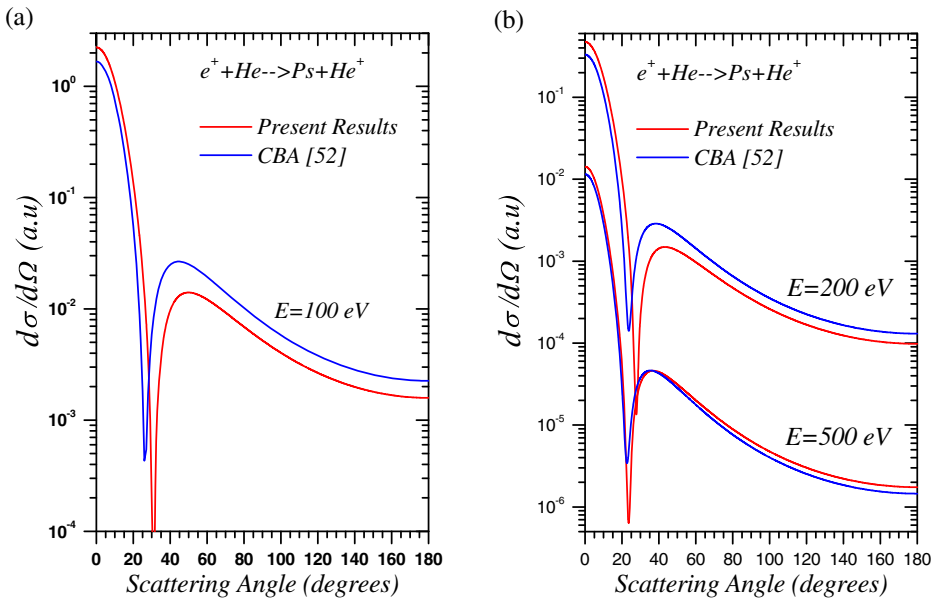

Fig. 1 (*Color online*) angular distribution of the differential cross sections for Ps formation from helium atoms

of the Coulomb–Born approximation (CBA) [51] for three impact energies: 100, 200, and 500 eV. In our computation, the dark angles, i. e., the angles at which cancelation occurs, are 31°, 28°, and 24°, while the CBA displays dark angles of 26°, 24°, and 23°, respectively. In both treatments, the dark angle becomes smaller as the incident energy grows.

Our results differ significantly from the CBA data at 100 eV incident energy. Below (above) 30° scattering angle, our differential cross sections are always smaller (larger) than the CBA results. As the impact energy increases, the difference between our results and the CBA results shrinks. Compared with the difference at 100 eV, the difference at 200 eV is smaller, and the difference at 500 eV is negligible. For energies above 500 eV, our results are consistent with the CBA results. Consequently, the total cross sections obtained from the two formalisms converge at high energies.

Figure 2 compares the total positronium formation cross sections obtained from our formalism with the experimental measurements of Diana et al. [36], Fromme et al. [37], Fornari et al. [38], Overton et al. [39], and Murtagh et al. [40] and also with the results of the CBA with $Z_T = 1.6875$, 2, and $\sqrt{-2\epsilon_i}$ [51] and of the two-center convergent close-coupling (CCC) formalism [18]. As Fig. 2a shows, our formalism yields reasonable agreement with experiment at energies above 50 eV in spite of its simplicity. Both the present approach and the CBA formalism [51] are based on perturbation expansion, an approach long known to be unreliable at low scattering energies.

For the first-order Born approximation to be accurate, the higher-order terms in the expansion series must be small in comparison with the first-order term. At high energies, since two-step scattering processes, such as the Thomas double-scattering mechanism, become dominant at high energies, the first-order approach yields poor approximations to the differential cross sections. All considered, we see that first-order methods are only reliable in a bracket of energies not so low as to render the perturbative method inapplicable and not so high as to make double-scattering mechanisms dominant.

Both the CBA and our approach satisfy the correct boundary conditions. The two methods are nonetheless nonequivalent: while the CBA breaks post–prior symmetry, our approach is symmetric, so that the initial and final wave functions associated with GSZ potential are consistent with the scattering potential and bound energies. Our approach is, hence, expected to be more appropriate to describe experimental processes. As the plots in Fig. 2b show, however, only small differences separate the CBA results from ours.

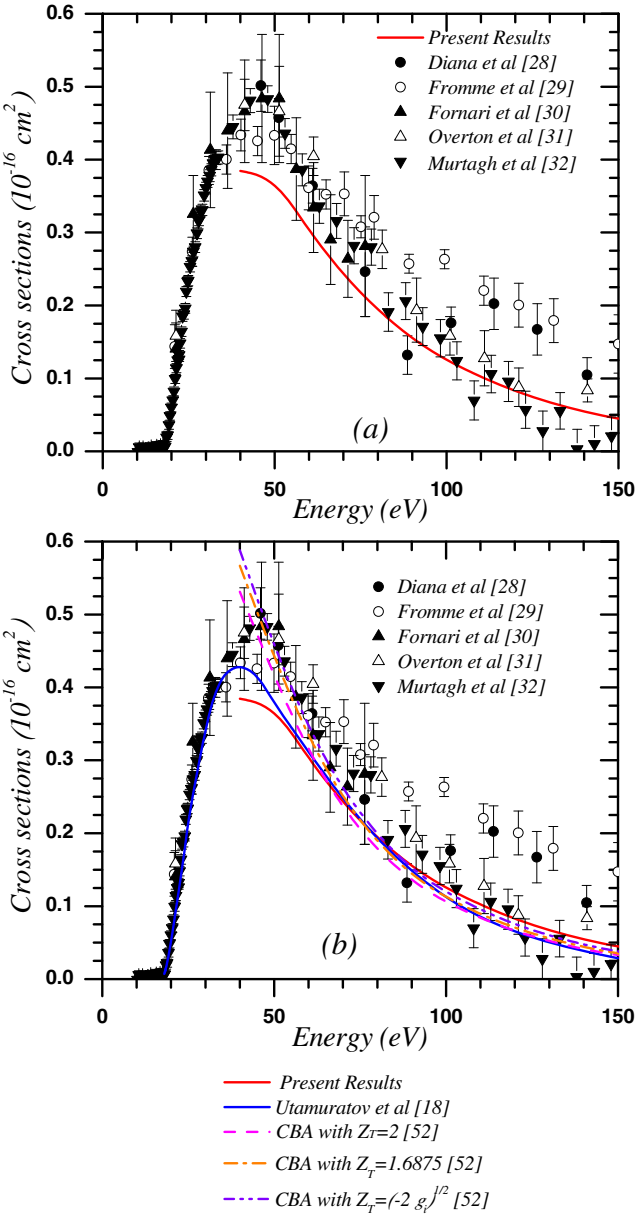

Fig. 2 (*Color online*) total cross sections for Ps formation in collisions of positrons with helium atoms, compared with the results of the listed theoretical and experimental studies

More accurate positronium formation cross sections are obtained with the CCC formalism, a more elaborate method employing a multiconfigurational wave function treatment to describe the He ground state. The accuracy of the calculated cross sections is controlled by the size of the basis and of the set quantum numbers of the included states at each center. Figure 2b shows good agreement between the CCC curve and the experimental data.

Within the energy bracket in which it is reliable, the solid line depicting our results in Fig. 2b agrees

with the CCC line. The difference between the two sets theoretical data is less than 0.7 % around 50 eV, while deviations of approximately 17 % separate the CBA and CCC curves in the same region. At higher energies, the results of the three formalisms converge and display good agreement with the experimental data.

Figure 3 compares various theoretical approaches with experiment. Cross sections calculated by the CBA with $Z_T = 1.6875$, 2 and $\sqrt{-2\epsilon_i}$ [51], the correct-boundary first-order Born (B1B) [32] formalism, the distorted-wave Born (DW) approximation [52], the continuum distorted-wave (CDW) approximation [33], and the close-coupling method (CC) [34] are compared with the experiments of Fornari et al. [38] and Overton et al. [39]. The CBA, CDW, and CC agree well with the measurements in the depicted energy range. The agreement between B1B and DW at high energies is fair, but at lower energies those theories deviate from the measurements.

Our predictions also deviate from experiment at low energies, but the agreement improves as the energy increases. Compared with the results of B1B and DW, our results are closer to the experimental data at low energies.

Figure 4 compares the above discussed theories with the earlier experimental measurements reported by Murtagh et al. [40]. The CDW, CC, and CBA formalisms yield results in very good agreement with experiment over the entire energy range. Our results are also in good agreement at energies above 75 eV, but the discrepancies are sizable at lower energies. The B1B and DW results are above the data by Murtagh et al. [40] for all energies lower than 200 eV; the deviation growing considerably as the impact energy decreases. Above 200 eV, all theories converge to the experimental data.

In addition to the CCC formalism, a number of theoretical descriptions of positronium formation in positron–helium atom collisions have been recently reported, on the basis of the momentum-space coupled-channel optical (CCO) method [19] and second-order distorted-wave approximation (DWA) [17]. Figure 5

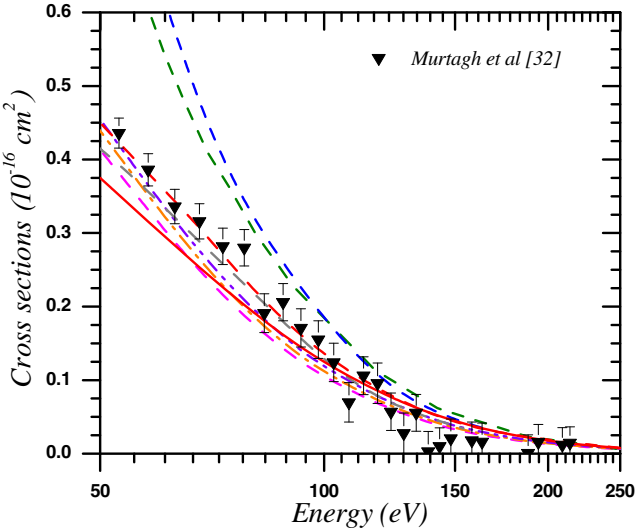

Fig. 4 (*Color online*) theoretical cross sections, as in Fig. 3, compared with the measurements by Murtagh et al. [40]

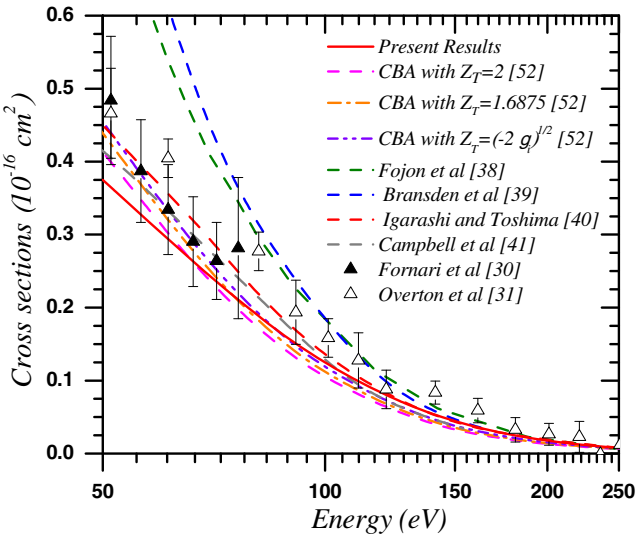

Fig. 3 (*Color online*) total cross sections, compared with the results of the CBA [51], B1B [32], DW [52], CDW [33], and CC [34] procedures and with the experimental data from Fornari et al. [38] and Overton et al. [39]

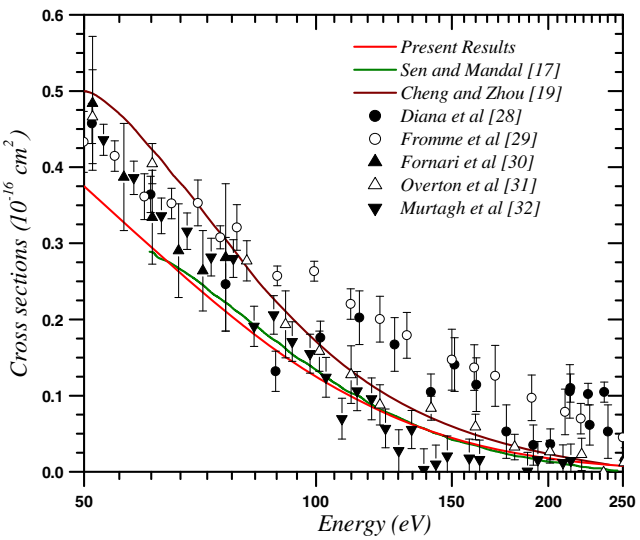

Fig. 5 (*Color online*) cross sections for positronium formation in helium atoms compared with all available experimental data and with the results of the DWA [17] and CCO [19] formalisms

compares our results in the energy range of 50–250 eV with the available results from the CCO and DWA formalisms, as well as with the experimental data reported by different groups [36–40]. Our first-order distorted wave results are very close to the predictions of the second-order DWA, in which the cross sections for Ps formation in the 1s orbital has been added to 1.66 times the Ps cross sections in the $n = 2$ orbitals to yield the total Ps formation cross sections.

Below 80 eV, our results underestimate the experimental cross sections. At small energies, all theories in the plot become inaccurate; the CCO cross sections overshooting the data by Murtagh et al. [40]. At relatively higher energies above 80 eV, our results agree with the other theoretical predictions and with the measurements.

Figure 6 shows the total positronium formation cross sections in our calculation formalism and all the above-mentioned theoretical calculations. Comparison with measurements reported by Murtagh et al. [40] identifies the CDW [33], CC [34], and CBA (with $Z = 2$) as the most reliable ones. As before, our data show only fair agreement with these three theories at low energies and good agreement at higher energies. Compared with the results of Fojón et al. [8] and of Bransden et al. [52], our results show substantially superior agreement with experiment low energies. In the considered range of impact energies, our results are compatible with those from the more complex CCC formalism.

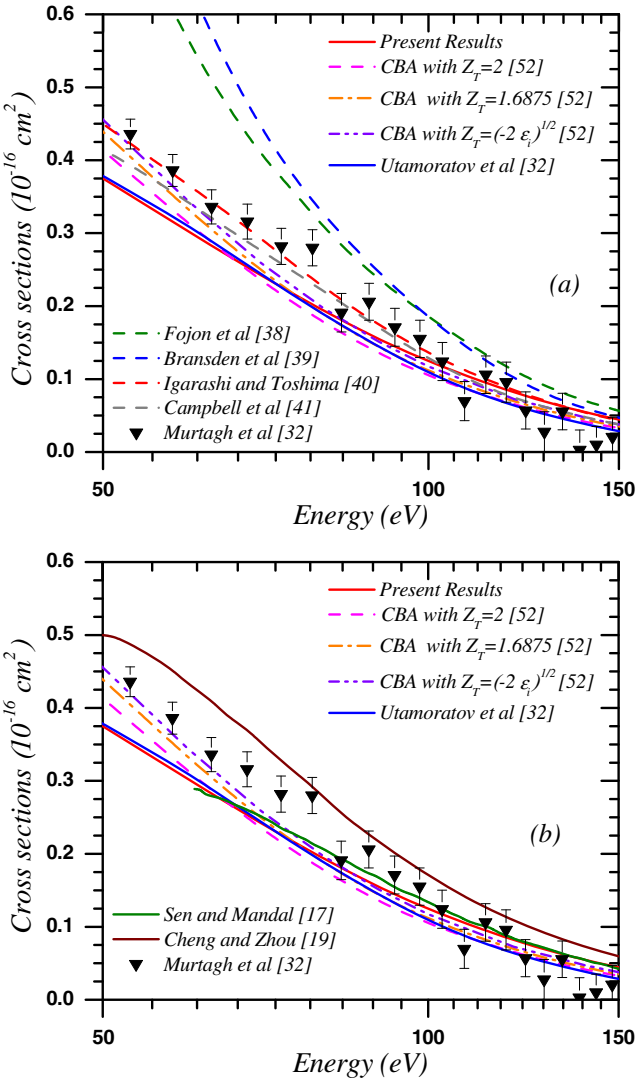

Fig. 6 (*Color online*) total cross sections for Ps formation from helium atoms compared the results of the listed theories and with the experimental data by Murtagh et al. [40]

4 Summary and Conclusions

In summary, we have applied a first-order distorted wave with correct boundary conditions to positronium formation from helium atoms. A parameterized potential in good agreement with Roothaan–Hartree–Fock wave function and the corresponding binding energy described the screening effect of the passive electron on the transition amplitude. Our theory is self-consistent since it satisfies the correct boundary conditions and the post–prior symmetry and since the interaction potentials, wave functions, binding energies, and Coulomb phase factors in the formalism are consistent with each other and describe the collision and electron capture realistically.

The chief advantage of our approach is its simplicity. The figures in this paper comprehensively compare the results of this approach with different sets of experimental data and with the results of more elaborate theories. They therefore set benchmarks monitoring the accuracy of the treatment. Compared with the results of the CBA, the angular distribution of our differential cross sections are in qualitative agreement even at the smallest energies: they differ quantitatively at the smallest energies, but the agreement improves as the impact energy grows.

Our calculated total cross sections are in reasonable agreement with other theories, such as the CBA, CDW, CC, CCO, and DWA, especially at higher energies. Also, the results agree well with the experimental data of Fornari et al. [38], Overton et al. [39], and Murtagh et al. [40], the agreement with the latter authors being very good at incident energies above 75 eV. As evidenced by comparison with experimental and other theoretical data, our procedure becomes less

accurate as the impact energy is reduced, with significant deviations becoming apparent around 50 eV.

Our relatively simple approach, based on the first-order distorted-wave formalism , reproduces the results of more demanding procedures based on the second-order distorted-wave approximation. It can be applied to positronium formation in multielectron atoms, such as C, Ne, Na, and Ar, and also to electron capture from atomic shells of multielectron atoms by bare ion projectiles at moderate energies.

Acknowledgements The author would like to thank Dr. Daniel Murtagh for providing the experimental data which were measured by his group (UCL positron group) on the different positron scattering processes from helium atoms and to Dr. Ravshan Utamoratov for forwarding his results for Ps formation based on the two-center convergent close-coupling formalism in tabular form.

References

1. M. Charlton, J.W. Humberston, *Positron Physics* (Cambridge University Press, Cambridge, 2001)
2. C.M. Surko, F.A. Gianturco, *New directions in antimatter chemistry and physics* (Kluwer Academic, Dordrecht, 2001)
3. Y.C. Jean, P.E. Mellon, Schrader D M, *Principles and applications of positron and positronium chemistry* (World Scientific Publishing Company, Singapore, 2003)
4. J.M. Puska, R.M. Nieminen, Rev. Mod. Phys. **66**, 841 (1994)
5. A. David, G. Kögel, P. Sperr, W. Triftshäuser, Phys. Rev. Lett. **87**, 067402 (2001)
6. G. Jerusalem, R. Hustinx, Y. Beguin, G. Fillet, Eur. J. Cancer **39**, 1525 (2003)
7. G.F. Gribakin, J. Ludlow, Phys. Rev. A **70**, 032720 (2004)
8. O. Fojón, J. Hanssen, P.A. Hervieux, R.D. Rivarola, J. Phys. B: At. Mol. Opt. Phys. **33**, 3093 (2000)
9. G. Laricchia, S. Brawley, D.A. Cooke, Á. Kövér, D.J. Murtagh, A.I. Williams, J. Phys.: Conference Series **194**, 012036 (2009)
10. D.A. Cooke, D.J. Murtagh, G. Laricchia, J. Phys.: Conference Series **199**, 012006 (2010)
11. L.J.M. Dunlop, G.F. Gribakin, Nucl. Instrum. Methods Phys. Res. B **247**, 61 (2006)
12. P.A. Macri, R.O. Barrachina, Nucl. Instrum. Methods Phys. Res. B **266**, 393 (2008)
13. P.A. Macri, R.O. Barrachina, Nucl. Instrum. Methods B **267**, 366 (2009)
14. Caradonna P, Sullivan J P, Jones A, Makochekanwa C and Buckman S J 2009 Phys. Rev. A **80** 060701
15. E. Surdutovich, J.M. Johnson, W.E. Kauppila, C.K. Kwan, T.S. Stein, Phys. Rev. A **65**, 032713 (2002)
16. E. Surdutovich, M. Harte, W.E. Kauppila, C.K. Kwan, T.S. Stein, Phys. Rev. A **67**, 022709 (2003)
17. S. Sen, P. Mandal, Phys. Rev. A **80**, 062714 (2009)
18. R. Utamuratov, A.S. Kadyrov, D.V. Fursa, I. Bray, A.T. Stelbovics, J. Phys. B: At. Mol. Opt. Phys. **43**, 125203 (2010)
19. Y. Cheng, Y. Zhou, Phys. Rev. A **76**, 012704 (2007)
20. Y. Cheng, Y. Zhou, Phys. Rev. A **73**, 024701 (2006)
21. J.P. Marler, J.P. Sullivan, C.M. Surko, Phys. Rev. A **71**, 022701 (2005)
22. A.T. Le, M.W.J. Bromley, C.D. Lin, Phys Rev A **71**, 032713 (2005)
23. G. Nan, Y. Zhou, Y. Ke, Phys. Rev. A **72**, 012709 (2005)
24. D.J. Murtagh, D.A. Cooke, G. Laricchia, Phys. Rev. Lett. **102**, 133202 (2009)
25. Y. Ke, Y. Zhou, G. Nan, Phys. Rev. A **70**, 024702 (2004)
26. W.E. Kauppila, E.G. Miller, H.F.M. Mohamed, K. Pipinos, T.S. Stein, E. Surdutovich, Phys. Rev. Lett. **93**, 113401 (2004)
27. R.N. Hewitt, C.J. Noble, B.H. Bransden, J. Phys. B: At. Mol. Opt. Phys. **25**, 557 (1992)
28. N.K. Sarkar, M. Basu, A.S. Ghosh, Phys. Rev. A **45**, 6887 (1992)
29. D.R. Schultz, R.E. Olson, Phys. Rev. A **38**, 1866 (1998)
30. P. Mandal, S. Guha, N.C. Sil, J. Phys. B: At. Mol. Phys. **12**, 2913 (1979)
31. P. Van Reeth, J.W. Humberston, J. Phys. B: At. Mol. Opt. Phys. **32**, 3651 (1999)
32. O.A. Fojón, R. Gayet, J. Hanssen, R.D. Rivarola, Phys. Scr. **51**, 204 (1995)
33. A. Igarashi, N. Toshima, Phys. Lett. A **164**, 70 (1992)
34. C.P. Campbell, M.T. McAlinden, A.A. Kernoghan, H.R.J. Walters, Nucl. Inst. Meth. B **143**, 41 (1998)
35. M. Charlton, G. Clark, T.C. Griffith, G.R. Heyland, J. Phys. B: At. Mol. Phys. **16**, L465 (1983)
36. L.M. Diana, P.G. Coleman, D.L. Brooks, P.K. Pendleton, D.M. Norman, Phys. Rev. A **34**, 2731 (1986)
37. D. Fromme, G. Kruse, W. Raith, G. Sinapius, Phys. Rev. Lett. **57**, 3031 (1986)
38. L.S. Fornari, L.M. Diana, P.G. Coleman, Phys. Rev. Lett. **51**, 2276 (1983)
39. N. Overton, R.J. Mills, P.G. Coleman, J. Phys. B: At. Mol. Opt. Phys. **26**, 3951 (1993)
40. D.J. Murtagh, M. Szłuińska, J. Moxom, P. Van Reeth, G. Laricchia, J. Phys. B: At. Mol. Opt. Phys. **38**, 3857 (2005)
41. F. Decker, J. Eichler, Phys. Rev. A **39**, 1530 (1989)
42. A.E.S. Green, D.L. Sellin, A.S. Zachor, Phys. Rev. **184**, 1 (1969)
43. P.P. Szydlik, A.E.S. Green, Phys. Rev. A **9**, 1885 (1974)
44. N. Toshima, T. Ishihara, J. Eichler, Phys. Rev. A **36**, 2659 (1987)
45. Dž. Belkić, S. Saini, H.S. Taylor, Z. Phys. D **3**, 59 (1986)
46. E. Clementi, C. Roetti, At. Data Nucl. Data Tables **14**, 177 (1974)
47. R.R. Lewis Jr., Phys. Rev. **102**, 537 (1956)
48. R.P. Feynman, Phys. Rev. **76**, 769 (1949)
49. J.R. Oppenheimer, Phys. Rev. A **31**, 349 (1928)
50. Y.B. Band, Phys. Rev. A **8**, 243 (1973)
51. E. Ghanbari-Adivi, Eur. Phys. J. D **62**, 389 (2011)
52. B.H. Bransden, C.H. Joachain, J.F. McCann, J. Phys. B : At. Mol. Opt. Phys. **25**, 4965 (1992)